Top ten European heatwaves since 1950 and their occurrence in the coming decades

2015 Environ. Res. Lett. 10 124003

(http://iopscience.iop.org/1748-9326/10/12/124003)

Environmental Research Letters

LETTER

Top ten European heatwaves since 1950 and their occurrence in the coming decades

Simone Russo[1,2], **Jana Sillmann**[3] **and Erich M Fischer**[4]

[1] European Commission, Joint Research Centre, Ispra, Italy
[2] Institute for Environmental Protection and Research (ISPRA), Rome, Italy
[3] Center for International Climate and Environmental Research (CICERO), Pb. 1129 Blindern, N-0318 Oslo, Norway
[4] Institute for Atmospheric and Climate Science, ETH Zurich, Universitatstrasse 16, 8092 Zurich, Switzerland

E-mail: simone.russo@jrc.ec.europa.eu

Keywords: heat wave magnitude index daily, extreme temperatures, European heatwaves, heat wave magnitude unit, Russian heatwave, Finland heatwave, heatwave projections

OPEN ACCESS

RECEIVED
25 August 2015

REVISED
20 October 2015

ACCEPTED FOR PUBLICATION
2 November 2015

PUBLISHED
27 November 2015

Abstract

The Russian heatwave in 2010 killed tens of thousands of people, and was by far the worst event in Europe since at least 1950, according to recent studies and a novel universal heatwave index capturing both the duration and magnitude of heatwaves. Here, by taking an improved version of this index, namely the heat wave magnitude index daily, we rank the top ten European heatwaves that occurred in the period 1950–2014, and show the spatial distribution of the magnitude of the most recent heatwave in summer 2015. We demonstrate that all these events had a strong impact reported in historical newspapers. We further reveal that the 1972 heatwave in Finland had a comparable spatial extent and magnitude as the European heatwave of 2003, considered the second strongest heatwave of the observational era. In the next two decades (2021–2040), regional climate projections suggest that Europe experiences an enhanced probability for heatwaves comparable to or greater than the magnitude, extent and duration of the Russian heatwave in 2010. We demonstrate that the probability of experiencing a major European heatwave in the coming decades is higher in RCP8.5 than RCP4.5 even though global mean temperature projections do not differ substantially. This calls for a proactive vulnerability assessment in Europe in support of formulating heatwave adaptation strategies to reduce the adverse impacts of heatwaves.

1. Introduction

Since 1950 large areas across Europe have experienced many intense and long heatwaves producing notable impacts on human mortality, regional economies, and natural ecosystems (Meehl and Tebaldi 2004, Schär *et al* 2004, García-Herrera *et al* 2010). So far it has been difficult to compare them across regions, because temperatures considered as normal by people accustomed to hotter climates can be categorized as heatwave in cooler areas if they are outside the area's normal temperature range (Lass *et al* 2011). This problem has been overcome by percentile-based indices (Alexander *et al* 2006) and by the novel heat wave magnitude index (HWMI, Russo *et al* 2014) summing up the excess temperatures beyond a certain normalized threshold and merging duration and temperature anomaly of intense heat events into a single number. This enables comparison of heatwaves with different length and peak magnitudes that have occurred in different regions and in different years (Hoag 2014).

However, in this study we show that the HWMI has some limitation in assigning magnitude to very high temperatures in particular in a changing climate. More precisely, the one-to-one correspondence between the sum of temperature of three consecutive hot days (sub-heatwave) and probability saturates when a sub-heatwave is composed by days with temperature values exceeding the highest temperature recorded during the reference period 1981–2010. The problem of saturation could results in an underestimation of heatwave magnitude in a warming climate. To overcome this problem, the HWMI has been

replaced by the heat wave magnitude index daily (HWMId) using a different formula in assigning magnitude to a single day composing a heatwave. Here we demonstrate the strength of the HWMId in classifying heatwaves, by identifying several historical heatwave events across Europe based on gridded daily temperature observations. The fact that all events were well documented in the news illustrates that, in contrast to some previous indices, HWMId captures events that are perceived as heatwaves by a broader public.

As documented in many studies (Schär *et al* 2004, Beniston *et al* 2007, Fischer and Schär 2010, Barriopedro *et al* 2011, Stott *et al* 2011, Sillmann *et al* 2013, Russo *et al* 2014), the increase in global surface temperature is expected to alter the magnitude and the frequency of heatwave events also in Europe by the end of the century. At a global scale, area affected by heat extremes is projected to increase already in the next decades (Battisti and Naylor 2009, Coumou and Robinson 2013, Fischer *et al* 2013) at a rate that is strongly dependent on the emission scenario already by mid-century. Here we focus on Europe and investigate whether such near-term changes in the occurrence of major heatwaves are also projected for Europe and whether the difference between different representative concentration pathways (RCPs) scenarios are noticeable also at the European scale.

We estimate the magnitude and the probability of occurrence of extreme heatwaves in the near-term (2020–2040), based on the HWMId from ten EURO-CORDEX regional climate projections under two different RCPs (RCP4.5 and RCP8.5). Thereby we investigate the area affected by heatwaves such as the ones experienced in the last decades and assess how they are affected by different RCPs.

2. Material and methods

2.1. Heat-wave magnitude index daily (HWMId)

The HWMId, is an improvement of the HWMI defined in Russo *et al* (2014). It is defined as the maximum magnitude of the heatwaves in a year; where:

Heatwave: period $\geqslant$3 consecutive days with maximum temperature (Tmax) above the daily threshold for the reference period 1981–2010. The threshold is defined as the 90th percentile of daily maxima temperature, centered on a 31 day window. Hence, for a given day *d*, the threshold is the 90th percentile of the set of data A_d defined by

$$A_d = \bigcup_{y=1981}^{2010} \bigcup_{i=d-15}^{d+15} T_{y,i}, \quad (1)$$

where $\bigcup$ denotes the union of sets and $T_{y,i}$ is the daily Tmax of the day *i* in the year *y*;

HWMId magnitude: sum of the magnitude of the consecutive days composing a heatwave, with daily magnitude calculated as follow:

$$M_d(T_d) = \begin{cases} \dfrac{T_d - T_{30y25p}}{T_{30y75p} - T_{30y25p}} & \text{if } T_d > T_{30y25p} \\ 0 \quad \text{if } T_d \leqslant T_{30y25p} \end{cases} \quad (2)$$

with T_d being the maximum daily temperature on day d of the heatwave, T_{30y25p} and T_{30y75p} are, the 25th and 75th percentile values, respectivelly, of the time series composed of 30 year annual Tmaxs within the reference period 1981–2010.

By definition the slope of the $M_d(T_d)$ is defined at each specific location depending on T_{30y75p} and T_{30y25p} which are different in places with different climates.

HWMId unit: the denominator of the Md function, defined as the difference between T_{30y75p} and T_{30y25p} (see equation (2)), is the inter quartile range (IQR) of the 30 yearly Tmaxs within the reference period 1981–2010. At each specific location, it represents a non-parametric measure of the variability of the time series composed by annual Tmaxs in 1981–2010. If a day of a heatwave has a temperature value $Td = T_{30y75p}$ its corresponding magnitude value calculated by means of the Md funtion will be equal to one. Hence, a daily heatwave magnitude unit is equivalent to that of a day with temperature T_{30y75p} and a corresponding anomaly equal to the IQR of the yearly maximua in 1981–2010. According to this definition, if the magnitude on the day d is 5, it means that the temperature anomaly on the day d with respect to the T_{30y25p} is 5 times the IQR which is the definite predetermined heatwave magnitude unit.

2.2. HWMId applied to daily minimum temperature (Tmin)

The definition of heatwave given in section 2.1, as done in many other studies (e.g. Frich *et al* 2002, Alexander *et al* 2006), is based on daily Tmax. However, during a heat event, an impact-relevant measurament of the heatwave magnitude takes into account also the cooling effect during the night (Perkins and Alexander 2013). In this study we compare the heatwaves defined through Tmax with the ones defined by means of the HWMI applied to daily Tmin calculated as the HWMId but with Tmin instead of Tmax.

2.3. HWMId versus HWMI

As reported in Russo *et al* (2014) the HWMI definition is based on the division of a heatwave to sub-heatwaves. A sub-heatwave is defined as period of three consecutive days above the daily threshold. The sum of three daily Tmaxs of a sub-heatwave are transformed in probability values (sub-heatwave magnitude) by means of the empirical cumulative distribution function (ECDF) function (see figure 1(b)). In the HWMI the magnitude of a heatwave was defined as the sum of the magnitudes of the n sub-heatwaves and the score of the HWMI was given by the maximum magnitude of all heatwave magnitudes for a given year. The HWMId differs from the previous HWMI version (Russo *et al* 2014) for two main improvements:

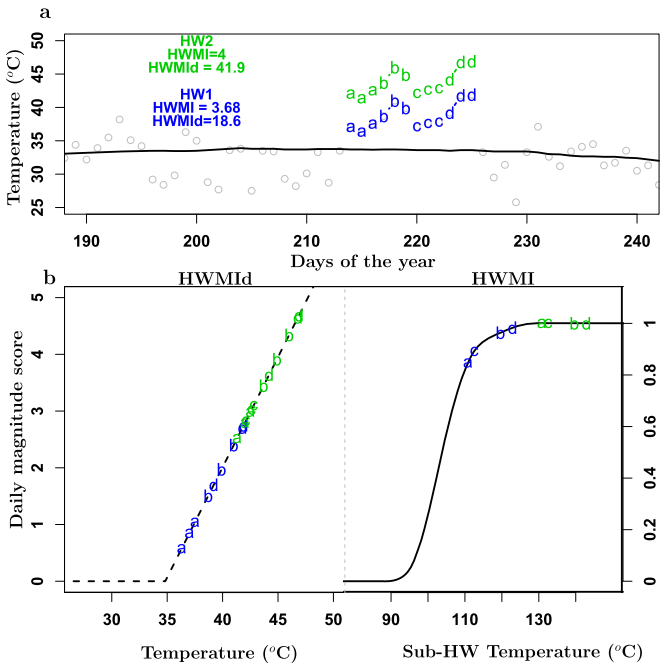

Figure 1. HWMId and HWMI calculation at a station in Carcassonne (Southern France). (a) E-OBS time serie of the year 2003 of daily maximum temperature in Carcassonne located in Southern France (open gray circles and blue letters) and daily threshold (black line). The blue letters, represent the daily maximum temperature values of the 2003 heatwave experienced in Carcassonne and indicated as HW1. The green letters, are the daily maximum temperature values of the HW2 heatwave obtained by adding 5 °C to each temperature of the 2003 heatwave HW1. As HW1, HW2 is composed by 4 sub-heatwaves represented by green letters a, b, c, d. (b) The dashed black line is the M_d function used to calculate the HWMId daily magnitude (see equation (2)), the black line denotes the empirical distribution of the sum of the three highest consecutive daily maximum temperatures of each year within the reference period 1981–2010 used in the HWMI calculation (see Russo *et al* 2014). Blue and green letters refer to each single day (left) or to each sub-heatwave (right) of the HW1 and HW2 heatwaves, respectively.

(i) the division in sub-heatwaves is not necessary

(ii) the daily magnitude is assigned by the M_d function with values in $[0, +\infty[$ and not in a bounded interval $[0, 1]$ as for the ECDF used in the HWMI.

Figure 1 shows a schematic example on the calculation and comparison of the HWMId and HWMI for two heatwaves with a duration of twelve days: one indicated as HW1 occurred in Carcassone (Southern France) in the summer of the 2003, and a second namely HW2 definded by adding 5 °C at each temperature value of HW1. Both heatwaves are composed by twelve days grouped into four sub-heatwaves of three days each (a, b, c, and d letters in figure 1). The R code used to reproduce the example above has been recently included in the 'hwmi' and 'hwmid' functions of the R package called 'extRemes' (Gilleland and Katz 2011). By using the 'hwmi' and 'hwmid' functions it is possible to reproduce all the calculations illustrated in this study. As already discussed above the HWMI, which has been the first climate indicator merging duration and magnitude of temperature anomalies of heat events into a single number, has some limitaion on measuring the magnitude of sub-heatwaves composed by high temperature values. In particular, all the sub-heatwaves of HW2, even if composed by days with different temperatures greater than the maximum value of the summer 2003 in Carcassone, have the same magnitude, corresponding to the saturation value of 1 (see figures 1(a) and (b)). Any other sub-heatwave with days warmer than the days of the HW2 sub-heatwaves will still have a magnitude of one. This problem has been overcome by the HWMId using the non-bounded and increasing monotonic function $M_d(T_d)$ in equation (2) assigning greater magnitude to the days of the HW2 with higher temperature (see figures 1(a) and (b)).

2.4. Models and observations

Daily maximum and minimum for continental surface temperature data from a gridded version (E-OBS 11.0) of the European Climate Assessment & Data (Haylock *et al* 2008, ECA&D, www.ecad.eu) are applied to study heatwaves in the present climate. The E-OBS is based on a grid resolution of $0.25^\circ \times 0.25^\circ$ and the data spans from 1950 to September 2015.

This data set is unique in its spatial extent, resolution and the use of many more European observing stations than in other European or global sets (Haylock *et al* 2008). For future projections (period 2006–2040) we used daily maximum and minimum temperature from 10 high-resolution (0.11°) regional climate model (RCM) simulations of the EURO-CORDEX (COordinated Regional Downscaling EXperiment—European Domain) multi-model scenario experiment. The model output is interpolated on the E-OBS grid for comparison with the observations. In the set of simulations, six RCMs are driven by five different general circulation models forced with two representative concentration pathways (RCP4.5 and RCP8.5), adopted by the Intergovernmental Panel on Climate Change (IPCC) for its fifth Assessment Report (AR5, Christensen *et al* 2013). For the period between 1980 and 2005 historical simulations were used (Taylor *et al* 2012). In detail, the ensemble model output used in this study is composed of the following 10 simulations: four RCA model simulations (Swedish Meteorological and Hydrological Institute) forced with four global climate models (CNRM-CM5, EC-EARTH, IPSL-CM5A-MR, and MPI-ESM-LR); two COSMO-CLM simulations (CLM Community) driven by lateral boundary conditions of two global climate models (CNRM-CM5, and EC-EARTH); one simulation for RACMO (Royal Netherlands Meteorological Institute), and one for HIRHAM5 (Danish Meteorological Institute), driven by EC-EARTH global model; one for WRF33 (Institut National de l'Environnement Industriel et des Risques) forced with IPSL-CM5A-MR global model and one MPI-CSC (The Max Plank Institute, Climate Service Center) simulation with the MPI-ESM-LR. More information on these models and simulations may be found at http://euro-cordex.net/fileadmin/user_upload/eurocordex/EUROCORDEX-simulations.pdf. The HWMId was calculated for the period between 1981–2040 for all available simulations and results are shown for two time slices of 30 year: 1981–2010 and 2011–2040.

2.5. Percentage of spatial area in heatwave

The percentageland area fraction in a specific year-experiencing HWMId values greater than a given magnitude level (HWMId $\geqslant$ 3, 4, 5, … , 24, …) (figure 3(a)), is calculated with respect to the land area of the entire EURO-CORDEX domain. In the specific case of the Russian heatwave in 2010, which was partly outside the EURO-CORDEX domain, we only count the grid points that are inside the domain.

2.6. Probability density functions (PDFs) and ECDFs of percentage of spatial area in heatwave

To produce the PDFs in figure 3(b) of the yearly percentage land area with HWMId $\geqslant$ 15 we use a gaussian kernel density estimate R with only a very weak smoothing in order to have the same information one would see in a histogram (Fischer *et al* 2013). The ECDFs in figure 3(c) are derived by sorting the data and associating at each value a probability calculated as the ratio between the rank of the considered value and (N+1), where $N = 300$ (30 years X 10 models) is the total number of model years.

The same procedure described above has been used to calculate the ECDF at each HWMId level. The values of temperature anomaly shown in figure A2 are calculated at each grid point as the difference between the annual Tmax in a specific year and the mean value of the time series composed by 30 year annual maxima of the reference period 1981–2010.

2.7. Uncertainties and hypothesis testing

The calculation of the standard error of the empirical distribution shown in figure 3(c) and for the other ECDF composed by 300 points measuring the percentage of area with HWMId equal to or greater than a fixed level (HWMId $\geqslant$ 3, 4, 5, …), has been done by means of a bootstrap (Efron 1979). Given a set of N (in our case $N = 300$) model years, we draw 300 points with replacement from the data points and compute the median of the drawn sample. We repeat the procedure for 10 000 times. Finally, we summarize the resulting distribution using the median and the range of the set composed by 10 000 medians. The error bars (see figures 3(d), 4(b)) at each HWMId level are calculated as the range of the sample composed by 10 000 meadians. Moreover, we have used a Kolmogorov–Smirnov (K–S) test to verify the hypothesis that RCP8.5 has a stronger signal than RCP4.5 in spite of the short time horizon, and that RCP4.5 again has stronger heatwave magnitudes than the historical simulations.

2.8. Ranking method

The heatwave ranking method used in this study is based on two different aspects: the percentage of area at different HWMId levels (3, 4, 5, 6, etc …) and the HWMId peak. Given two heatwaves HW0 and HW1, HW0 is greater than HW1 if the percentage of area across all HWMId levels, is greater than that of HW1.

Where the ranking is not consistent across all HWMId levels we rank the heatwaves by the HWMId peak value.

3. Heatwave ranking since 1950

Figure 2(a) reports the historical newspaper quotes on the strongest European heatwaves since 1950 identified here and shows the corresponding geographical pattern of the HWMId, from the Ensembles-

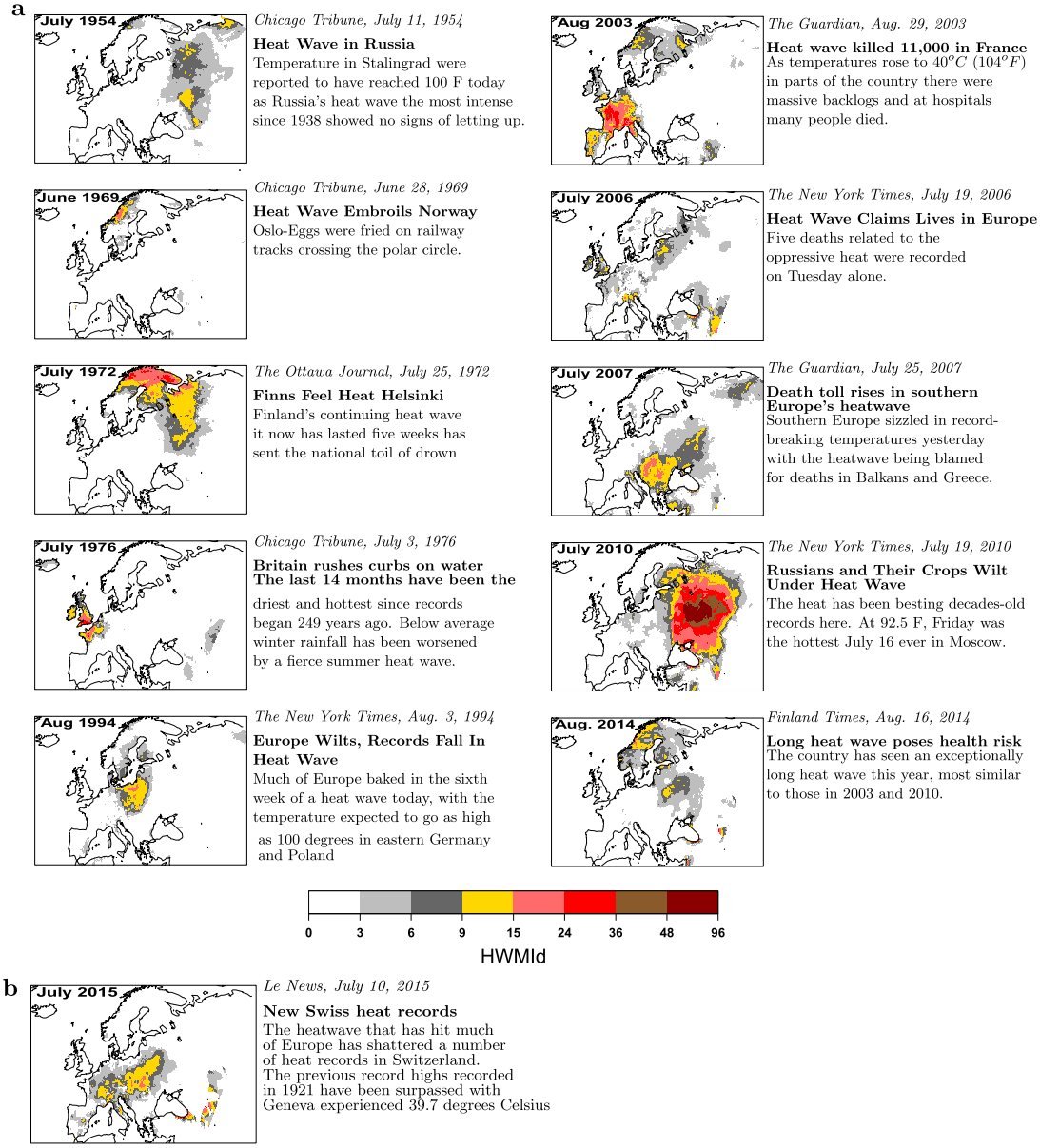

Figure 2. (a) Spatial distribution of the HWMId observed (E-OBS) values and spotted news of the top 10 European heatwaves since 1950; following the definition in section 2.1, at each grid point, the HWMId values represent the yearly maximum magnitude. (b) HWMId estimation with EOBS data from January to September 2015 for the most recent heatwave.

OBServations gridded dataset (E-OBS) (Haylock *et al* 2008). The fact that all the heatwaves identified here were covered in newspaper articles illustrates that the index captures events that are perceived as extreme heatwaves by the general public. Similar patterns are obtained by using the HWMI (figure A1) and the HWMId applied to Tmin (figure A2), the latter confirming the severity of most of these heatwaves which have been characterized by the persistence of extremely high night-time temperatures. The ranking of the most severe heatwaves has been done by following the criterium in section 2.8.

The first extreme event in this observational record occurred in 1954 in Russia when daily Tmaxs reached 38 °C (*Chicago Tribune*, 11 July 1954). We find that the highest HWMId values during this event were confined to Southern Russia (figure 2(a)) with maximum values recorded over the grid points with high heatwave anomaly and long persistence (figure A3). In 1969 temperatures were above normal over the polar circle with maximum values greater than 35 °C and HWMId peak equal to 26.5. 'Oslo-Eggs were fried on railway tracks crossing the polar circle. It was a pratical demonstration of an intense heatwave which has hit Norway for several weeks' (*Chicago Tribune*, 28 June 1969). However, this heatwave was characterized by comparatively cool nights with HWMId applied to Tmin exceeding the level of 3 only over a few locations in Norway (figure A2).

The magnitude of the extreme heatwave experienced in Finland in 1972 is comparable with that of the well-documented 2003 heatwave in Central Europe (Luterbacher *et al* 2004, Schär *et al* 2004, Fischer *et al* 2007, Vautard *et al* 2007, García-Herrera *et al* 2010, Barriopedro *et al* 2011, Stefanon *et al* 2012,

Table 1. List of record-breaking heatwave events in the period 1950–2014 with E-OBS data including also data until September 2015 for the most recent heatwave. The latter is an additional information to the originally considered top 10 heatwaves. For each specific event the spatial extent is estimated as the land area fraction exceeding a fixed HWMId value. The area fraction is expressed in percentage. The HWMId peak is the highest spatial HWMId value recorded during each specific event.

Year	Loc.	HWMId Peak	Area (%) HWMId $\geqslant 6$	Area (%) HWMId $\geqslant 9$	Area (%) HWMId $\geqslant 15$	Area (%) HWMId $\geqslant 24$
2010	Russia	71.9	36.38	29.13	22.54	14.07
2003	Cent. Eu	44.7	11.61	9.17	5.44	1.65
1972	Finland	38.2	26.42	18.35	6.57	0.96
1976	UK Brit.	35.8	4.55	2.98	1.21	0.23
1969	Norway	26.5	2.26	1.20	0.38	0.02
2015	Cent. Eu	26.0	11.94	5.67	0.56	0.01
2007	Greece	22.9	16.80	7.90	1.35	0
1994	Benelux	21.3	7.42	3.89	0.46	0
2014	Scandin.	21.2	11.58	3.65	0.3	0
1954	SW Rus.	19.7	9.3	1.9	0.05	0
2006	Cent. Eu	18.9	5.05	1.28	0.05	0

Miralles *et al* 2014, Russo *et al* 2014), but was not considered in previous catalogs of the strongest European heatwaves (Fischer *et al* 2007, Vautard *et al* 2007, Lass *et al* 2011, Stefanon *et al* 2012). According to news coverage the weather was exceptionally warm in summer 1972 in Finland with locations recording yearly Tmax anomalies greater than 8 °C and anomalously hot days persisting for more than 18 days (figure A3). An excess mortality of 840 deaths (2% of all annual deaths) in the summer of 1972 in Finland was directly attributable to the heatwave (Näyha 1981, 2007). The heatwave spatial extent, peak, and duration according to the HWMId were greater than the previous ones in 1954 and in 1969 (table 1 and figure 2(a)) and are comparable with the values of the heatwave in summer of 2003. In 1975–76 the UK experienced the famous drought that was memorable for its severity over most of the British Isles, and also for its exceptional persistence. In particular, in 1976 'the United Kingdom sweltered in temperatures exceeding 32.2 °C for 15 consecutive days. Further five days saw temperatures reaching 35 °C' (*The Telegraph,* 22 July 2011). During the night, as in Norway in 1969, the surface cooled rapidly, with HWMId values greater than 3 only over Southern UK and Northern France (figure A2).

Further major heatwaves are found across Europe (Italy 1983, UK 1983, Greece 1987, among others) but all of them were smaller in extent and with a lower HWMId spatial maximum than the top ten heatwaves presented in figure 2(a) and in table 1.

In 1994, The New York Times reported the headline: 'Europe Wilts, Records Fall In Heatwave'. The 1994 heatwave was most pronounced in Germany and Poland. Finally in the summer of 2003 the heat-related death toll was estimated between 20 000 and 70 000 people (Robine *et al* 2008, Barriopedro *et al* 2011, Christidis *et al* 2015). According to many studies the 2003 heatwave was the second strongest event in Europe since 1950 (Barriopedro *et al* 2011, Christidis *et al* 2015). Here we show that the spatial area extent in heatwave covered in 2003 was lower than that in 1972 at almost all HWMId levels (figures 2(a), 3(a), and table 1). On the contrary, in the 2003 the spatial area in heatwave during the night was greater than in 1972 at almost all HWMId levels (figures 4(a), A2). These two events had also comparable temperature anomalies and persistence of consecutive days above the 90th percentile threshold (figure A3).

Another event occurred in Europe in 2006. This heatwave had a few peaks spreading throughout Europe (figure 2(a)). In 2007 the 'death toll rises in Southern Europes heatwave' (*The Guardian*, see figure 2(a)). All of the previous records were broken in the 2010 in Russia during the worst European event in the observational era. It broke the night and day records in spatial extent, average, peak, and duration, in comparison with all the previous events. In particular, the 2010 Russian heatwave shows a spatial extent and a spatial HWMId maximum around double than that of the heatwave in Europe in 2003 and in Finland in 1972 (table 1, figures 2(a), 3(a), A2, A3).

Finally, in the 2014, as reported by Finland Times, 'The Met Office in a twitter feed on 25 July said the previous weeks mean temperature was the highest in the country for more than 50 years. The mean temperature in that period stood at 20.2 °C. Looking back at the statistics, the 26th week of 1972 was the warmest in the past 54 years'. (*Finland Times,* 11 August 2014). This is confirmed by the HWMId values showing that the Scandinavian heatwave occurred in 2014 was not as strong as the one that occurred in 1972.

3.1. The most recent European heatwave of summer 2015

The summer of the current year (2015) was very hot in Europe with an intense heatwave experienced by many countries. In Switzerland, Italy, Germany and part of Spain, the 2015 heatwave started in late June and at some location persisted for around 30 days until the end of July (see figure A3). In Austria, Slovakia, Croatia, Serbia, Romania, and Southern Ukraine the heat event started at the end of July and persisted till the first ten days of August (figure A3) The HWMId estimates for this heatwave have been

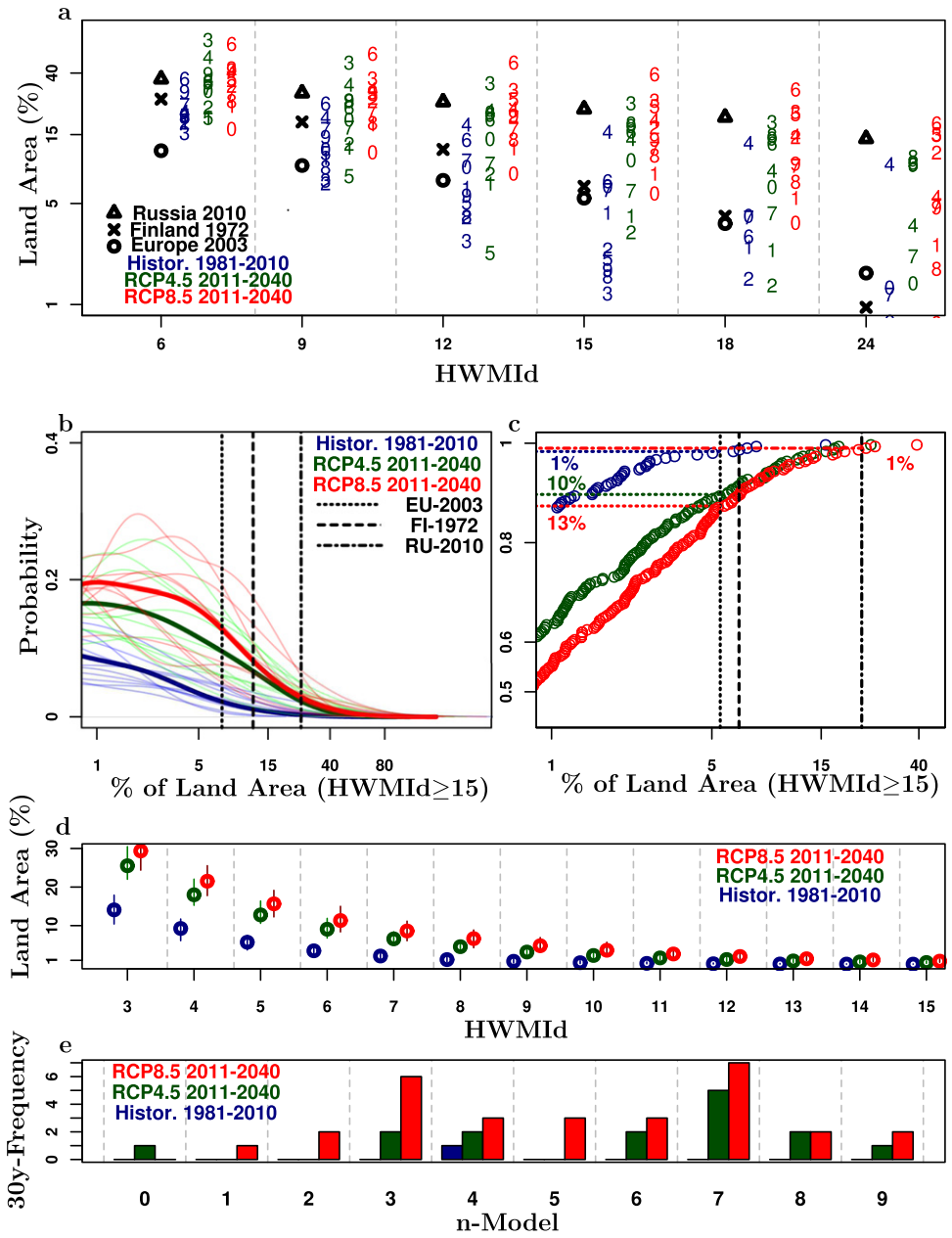

Figure 3. Empirical probability and cumulative distirbution functions (EPDFs and ECDFs) of the percentage land area in heatwaves. (a) Percentage of EURO-CORDEX land area covered by HWMId maximum values greater than a given magnitude level (HWMId $\geqslant$ 6, 9, … , 24) for the 2003, 1972, and 2010 European heatwaves with E-OBS data (black) and for the strongest heatwave simulated by each individual model in the periods 1981–2010 and 2011–2040. The numbers from 0 to 9 refer to heatwaves simulated by individual models (see table A.1). Hence, as an example, at each HWMId level the heatwave with the strongest magnitude and spatial extent simulated by the model 0, in 2011–2040 and under the RCP8.5 scenario, is represented by the red symbol 0. (b) PDFs of the percentage land area covered by grid points with HWMId values equal to or greater than 15. The PDFs are shown for the period 1981–2010 (blue curves) and 2011–2040 under RCP4.5 (green curves) and RCP8.5 (red curves) scenarios. The transparent couloured lines mark individual EURO-CORDEX models, comprised of 30 year values, whereas the bold colored curves represent the PDFs comprised of all 300 (30 years X 10 models) model years. Dotted and dashed lines denote the observed (E-OBS) 2003 and 2010 events, respectively. (c) As (b) but for ECDF of 300 model years. Each open circle represent the percentage of area (value on *x*-axis) and the corresponding probability for a single model year. The horizontal dashed and dotted lines denote the probability to have 2003 and 2010 type heatwave in 30 year period and under a specific scenario. (d) Percentage of area versus different HWMId levels. The open colored circles and the error bars represent the median and the range of the bootstrap applied at each HWMId level to the ECDF of 300 model years (see panel (c) for HWMId $\geqslant$ 15). (e) Occurrence of a 2003-type heatwave in present and near future periods of 30 year simulated by each model according to the ranking method in section 2.8.

done by using the E-OBS Tmax and Tmin data (see section 2.4) available until September 2015. According with the HWMId spatial distribution during the day (see figure 2(b) and table 1) this heatwave had lower magnitude than that occurred in the summer of 2003. Its largest anomaly and duration were recorded in Northern Italy and Swizerland (see figure A3) and its spatial extent at different HWMId levels was comparable withthe one of the heatwaves occurred in Greece in 2007, in central Europe in 1994 and in Scandinavian in 2014 (see table 1). Differently from these two events the heatwave of summer 2015 was characterized by a slow cooling during the night (see figure A2).

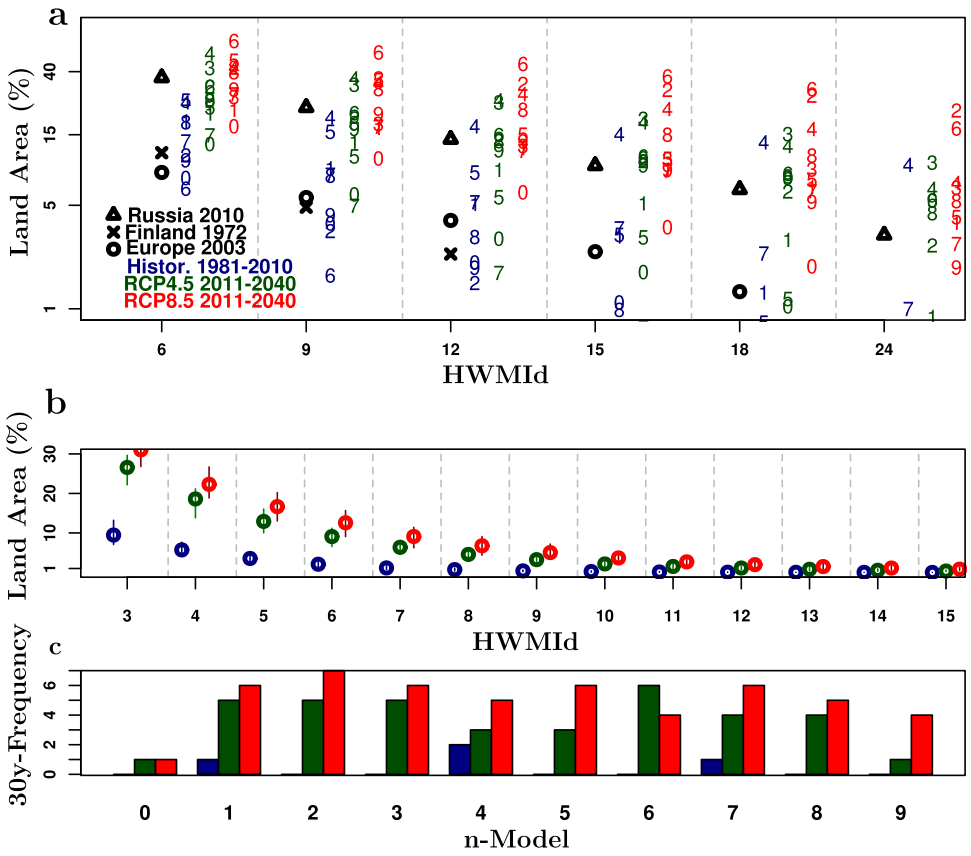

Figure 4. As figures 3(a), (d), (e) but for HWMId applied to Tmin (see section 2.2). (a) The strongest heatwave in 30 year period with Tmin simulated by each model (0, 1, 2, etc …) are coherent in space and time with those in figure 3(a). (For more details see also figures 5 and A4). (b) and (c) Colors indicate the same periods and scenarios as in figure 3(a).

4. Model evaluation (1981–2010)

We use an ensemble of 10 RCMs (see methods) to evaluate the simulated heatwave magnitude and extent against observations. Heatwaves in the same set of RCMs but driven by reanalysis data, have been evaluated in a recent study (Vautard *et al* 2013) showing that most models exhibit an overestimation of summertime observed temperature extremes in Mediterranian regions and an underestimation over Scandinavia. They show that if heatwaves in the model are defined with respect to the observed percentiles, their persistence is directly influenced by this bias. In fact, a model that overestimates the 90th percentile threshold of the simulated temperature with respect to the observations will show an obvious overestimation of heatwave duration. This effect is corrected in the previous study (Vautard *et al* 2013) and here by HWMId defining a heatwave as a period of consecutive hot days with daily Tmax above the 90th percentile threshold of the respective model and not with respect to the observations. The implicit bias correction included in HWMId calculation, gives high skill to this index in comparing heatwaves simulated by different climate models. All the models simulate heatwaves in northern, Southern, Eastern, and Western Europe and in particular over the regions where the top ten heatwaves occurred in the present (figure 5(a)).

But are the models able to simulate heatwaves of the magnitude of those in 2003 and 2010 to provide a reliable estimate of future summer climate (Beniston 2004, Fischer and Schär 2010, Diffenbaugh and Scherer 2011, Quesada *et al* 2012)? The simulated HWMId values in a thirty year period (1981–2010) representing present-day climate show that many models at different HWMId levels capture a 2003-type heatwave in the period 1981–2010, withonly one out of ten models simulating, at each HWMId level, a heatwave greater in spatial extent than observed in the 2003 (figures 3(a), 5(a): model4). The corresponding HWMId applied to Tmin for the heatwaves in figure 3(a) show similar results, with three out of ten models simulating, at each HWMId level, a heatwave greater in spatial extent than observed in the 2003 (figures 4(a) and (c), see models 1, 4, 7). None of the models is able to capture the spatial extent of the 2010 Russian heatwave at anyone of the HWMId level. (see figures 3(a), 5(a)). When using daily Tmin, only one model (figure 4(a), see model 4) at different magnitude levels shows a spatial area greater than that measured in the 2010.

5. Heatwaves in the next two decades

While global mean temperatures differ not substantially between the RCP8.5 and RCP4.5 scenarios in the

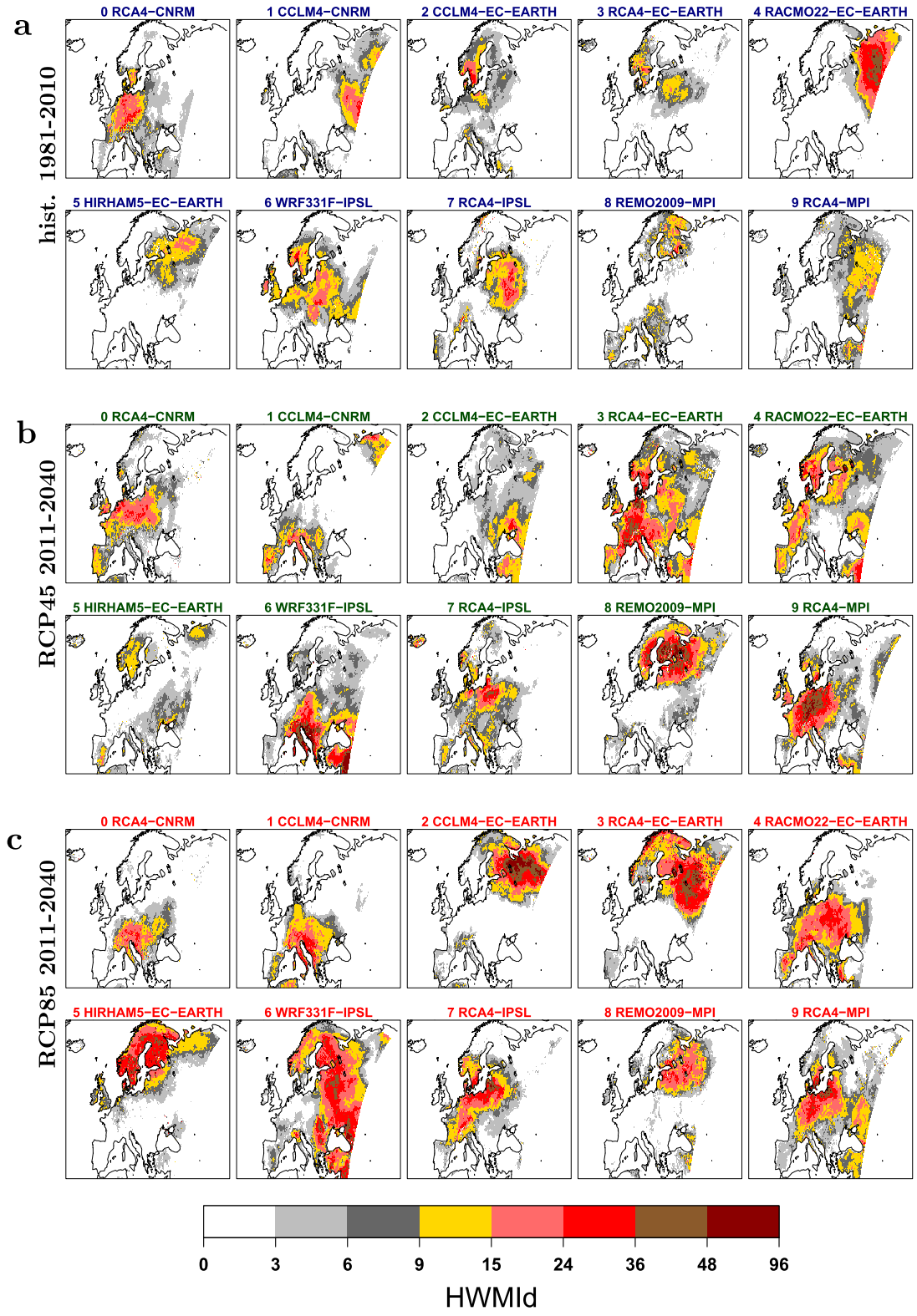

Figure 5. Spatial distribution of the HWMId values of the strongest heatwave in a 30 year period simulated by each of the ten models in a specific model-year. (a) present period (1981–2010) in the historical simulations (1981–2005) and RCP4.5 (2006–2010). (b) and (c) Next two decades (2011–2040) under the RCP4.5 and RCP8.5 scenarios, respectively.

coming two decades (Collins *et al* 2013) we find that the probability of experiencing a major European heatwave is increasing and is larger in theRCP8.5 than RCP4.5.

It is expected that along with warming temperatures a significant percentage of land fraction will see significantly more intense hot extremes (Clark *et al* 2006, Fischer *et al* 2013), with a probability of occurrence of extreme heatwaves increasing by a factor of 5 to 10 (Beniston *et al* 2007, Barriopedro *et al* 2011, Rahmstorf and Coumou 2011, Coumou and Robinson 2013, Christidis *et al* 2015). However,

Barriopedro *et al* (2011) have shown that the 2010 heatwave was so extreme that analogues will remain unusual for the next few decades under the A1B IPCC scenario (Christensen *et al* 2007). Likewise, we find that, following the ranking method in section 2.8 based on the HWMId calculated with daily Tmaxs, none of the 10 RCMs show a 2010-type heatwave in Europe under the RCP4.5 (Christensen *et al* 2013) (figure 2(a)), whereas three of the ten models show one under the RCP8.5 (figures 3(a), 5(c): models 3, 5, 6). These three heatwaves, at the same time and locations, show very high magnitude also during the night; with a percentage of area, measured at each magnitude level, greater than that recorded in Russia in the 2010 (figures 4(a), A4(c))

Moreover, almost all the models show that the probability of occurrence of an event like that of summer 2003 is expected to increase in the coming decades, occurring at least once in 30 year period under both RCP4.5 and RCP8.5 scenarios, (figures 3(a) and (e), 4(a) and (c), 5(b) and (c), A4). This signal, accordingly with at least 8 of the 10 models is greater under the RCP8.5 than the RCP4.5 (figures 3(e), 4(c)).

However, since we are using only one realization per GCM-RCM chain, we are not able to estimate a range of uncertainty expressing the likelihood of each single model in capturing a specific type of heatwave. Furthermore, note that in case that the absence of a 2010 heatwave in the period 1981–2010 is due to a model deficiency, the occurrence in the coming decades may also be biased low.

The PDF and the corresponding ECDF of the spatial area covered by grid points with HWMId equal to or greater than 15 (value exceeded by all the HWMId peak values of the top ten present heatwaves in table 1), show that in the next decades (2011–2040) the fraction of European area in heatwave is increasing with respect to the present-day period (1981–2010) under both the RCP4.5 and RCP8.5 scenarios (figures 3(b) and (c)). In order to test the uncertainties and the robustness of these rusults we have applied a bootstrap of 10 000 samples to the ECDFs calculated at each level of magnitude. The median and the range of the set composed by 10 000 ECDF medians versus the magnitude levels are represented in figures 3(d) and 4(b) for HWMId calculated with daily maximum and Tmins, respectively. The K–S test (see section 2.7) applied to the set composed by the 10 000 ECDF medians, calculated at each magnitude level, show that the null hypothesis that RCP4.5 is equal to the historical simulation is rejected at 1% level of significance in favor of the alternative hypothesis that RCP4.5 show a greater signal than historical simulations. The same test applied to the HWMId, with Tmax and Tmin data, in the coming decades shows that, at 1% level of significance, in the period 2011–2040 the expected percentage of area will be greater under the RCP8.5 than the RCP4.5 scenario, indicating that a small change in average global temperature leads to a dramatic change in intensity and frequency of extreme events (Karl *et al* 2008). Finally, in the very near future the strongest heatwave may occur anywhere in Europe (figures 5(b) and (c), A4(b) and (c)), indicating that respective adaptation strategies are needed in all European countries.

6. Conclusions

Our results provide a formal classification of the strongest heatwaves occurring in Europe since 1950, showing that according to our newly introduced metric the heatwave occurring in Finland in 1972 had larger spatial extent but smaller peak magnitude and duration as the one in 2003 in Central Europe. The RCMs show reasonable skill in simulating present-day extreme heatwaves, and indicate that anthropogenic increase in greenhouse gas concentrations implies an increased probability of extreme heatwaves in Europe in the next two decades (2021–2040). This enhanced probability of extreme heatwaves may regionally be masked or amplified by internal variability, which means that parts of Europe may experience a very rapid increase or no increase in heatwaves for 1–2 decades. However, in the long run heatwaves that are unusual in the current climate will become more common along with rising global mean temperatures and could occur in any country in Europe. Given the documented effects of the top ten heatwaves in the present, a high risk of associated adverse impacts in the near future is suggested. The new HWMId, which takes into account the severity of temperature extremes as well as the duration of the heatwave, and which also solves the saturation problem found in the HWMI, promises to be very useful in classifying future heatwaves and in providing significant information for adaptation strategies to decision-makers (Hoag 2014).

Acknowledgments

We acknowledge the E-OBS dataset from the EU-FP6 project ENSEMBLES (http://ensembles-eu.metoffice.com) and the data providers in the ECA&D project (http://ecad.eu). We acknowledge the Task Force for Regional Climate Downscaling (TFRCD) of the World Climate Research Programme (WCRP), which created the CORDEX initiative to generate regional climate change projections for Europe within the timeline of the Fifth Assessment Report (AR5) and beyond (http://euro-cordex.net/About-EURO-CORDEX.1864.0.html). JS is supported by ClimateXL (project no.243953) funded through the Norwegian Research Council.

Appendix

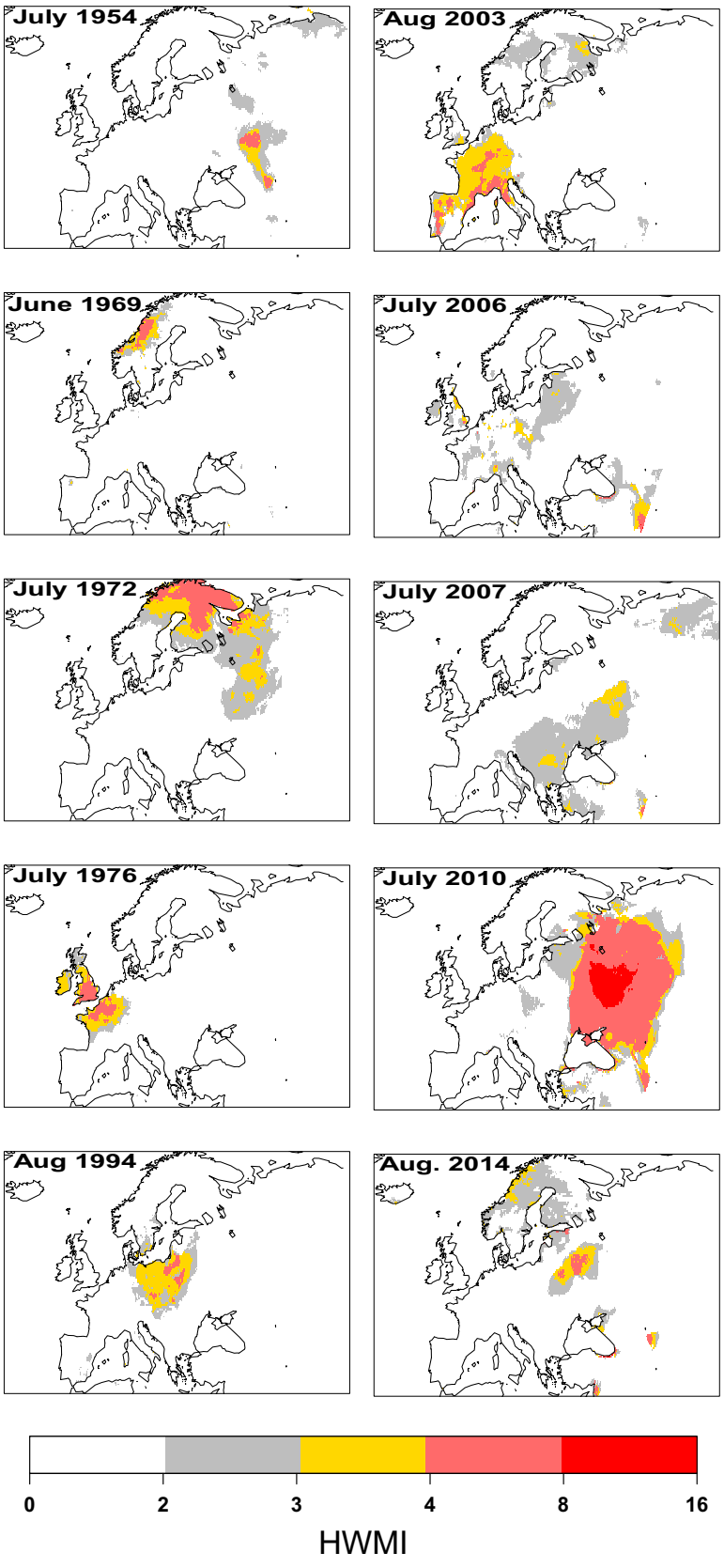

Figure A1. Spatial distribution of the HWMI observed (E-OBS) values of the top 10 European heatwaves since 1950.

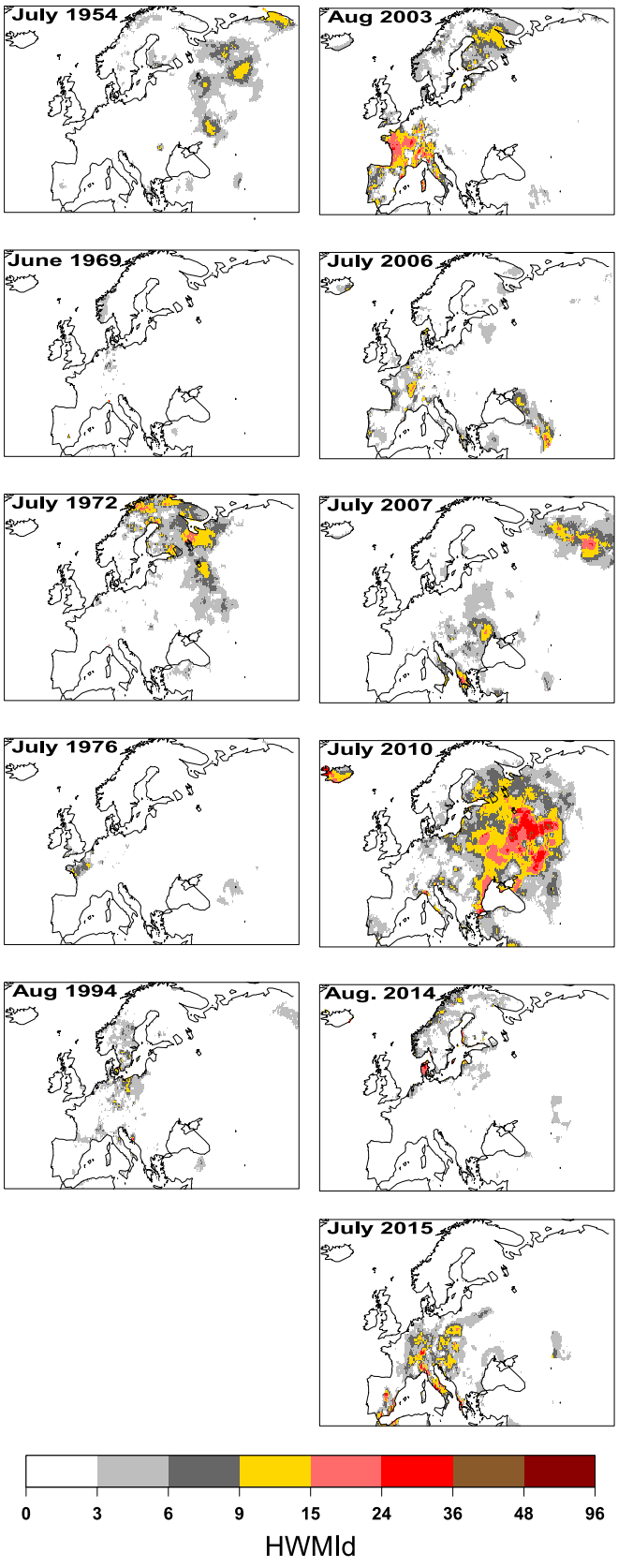

Figure A2. As figure 2 but for HWMId calculated with daily minimum temperatures.

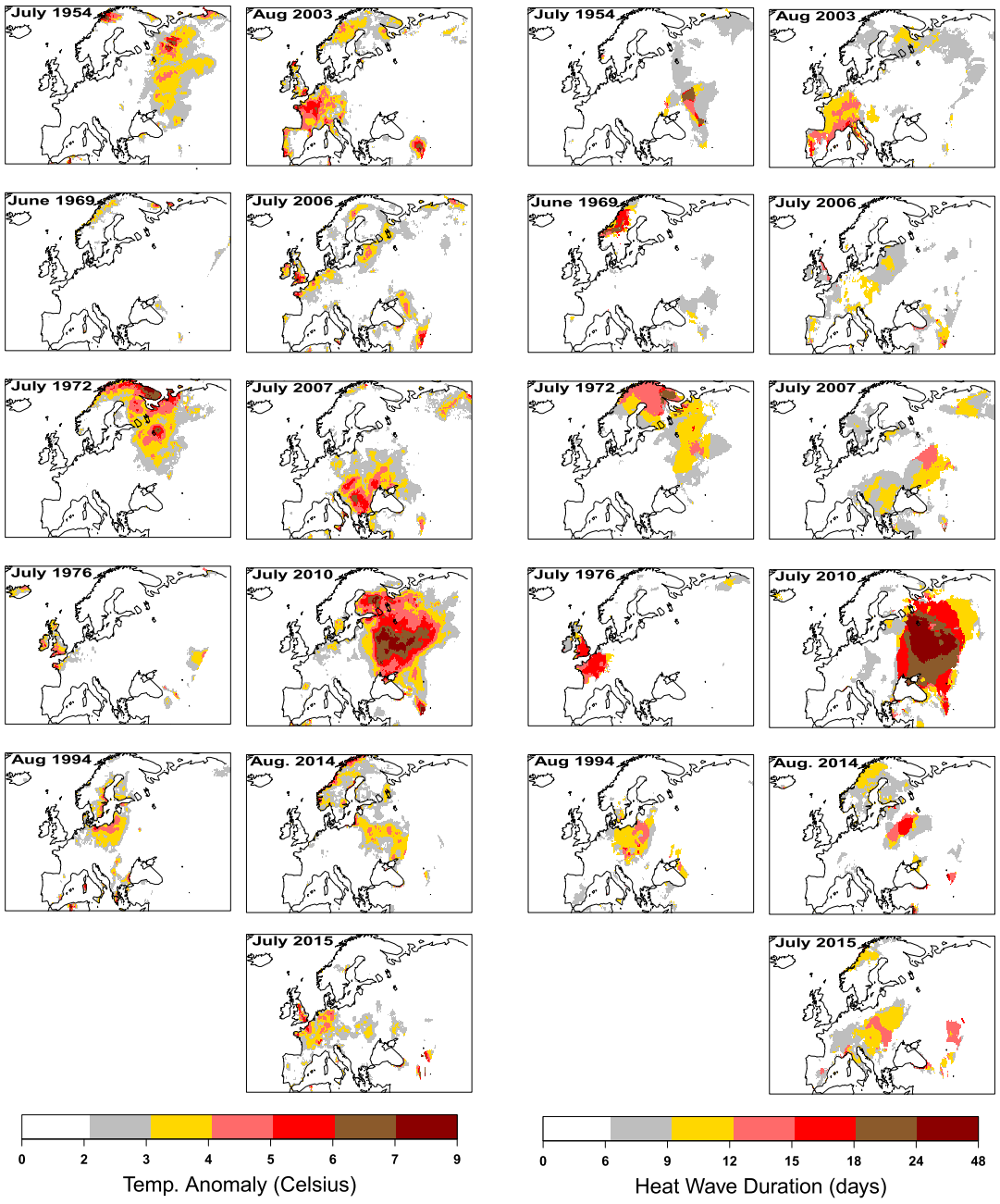

Figure A3. Temperature anomaly calculated following the definition in section 2.6 and heatwave duration of the top 10 European heatwaves and of the most recent heatwave of summer 2015.

Table A.1. List of the ten EURO-CORDEX used models.

Model number	Institute	RCM	Driving GCM
0	SMHI	RCA4	CNRM-CM5
1	CLMcom	CCLM4-8-17	CNRM-CM5
2	CLMcom	CCLM4-8-17	EC-EARTH
3	SMHI	RCA4	EC-EARTH
4	KNMI	RACMO22E	EC-EARTH
5	DMI	HIRHAM5	EC-EARTH
6	IPSL-INERIS	WRF331F	IPSL-CM5A-MR
7	SMHI	RCA4	IPSL-CM5A-MR
8	MPI-CSC	REMO2009	MPI-ESM-LR
9	SMHI	RCA4	MPI-ESM-LR

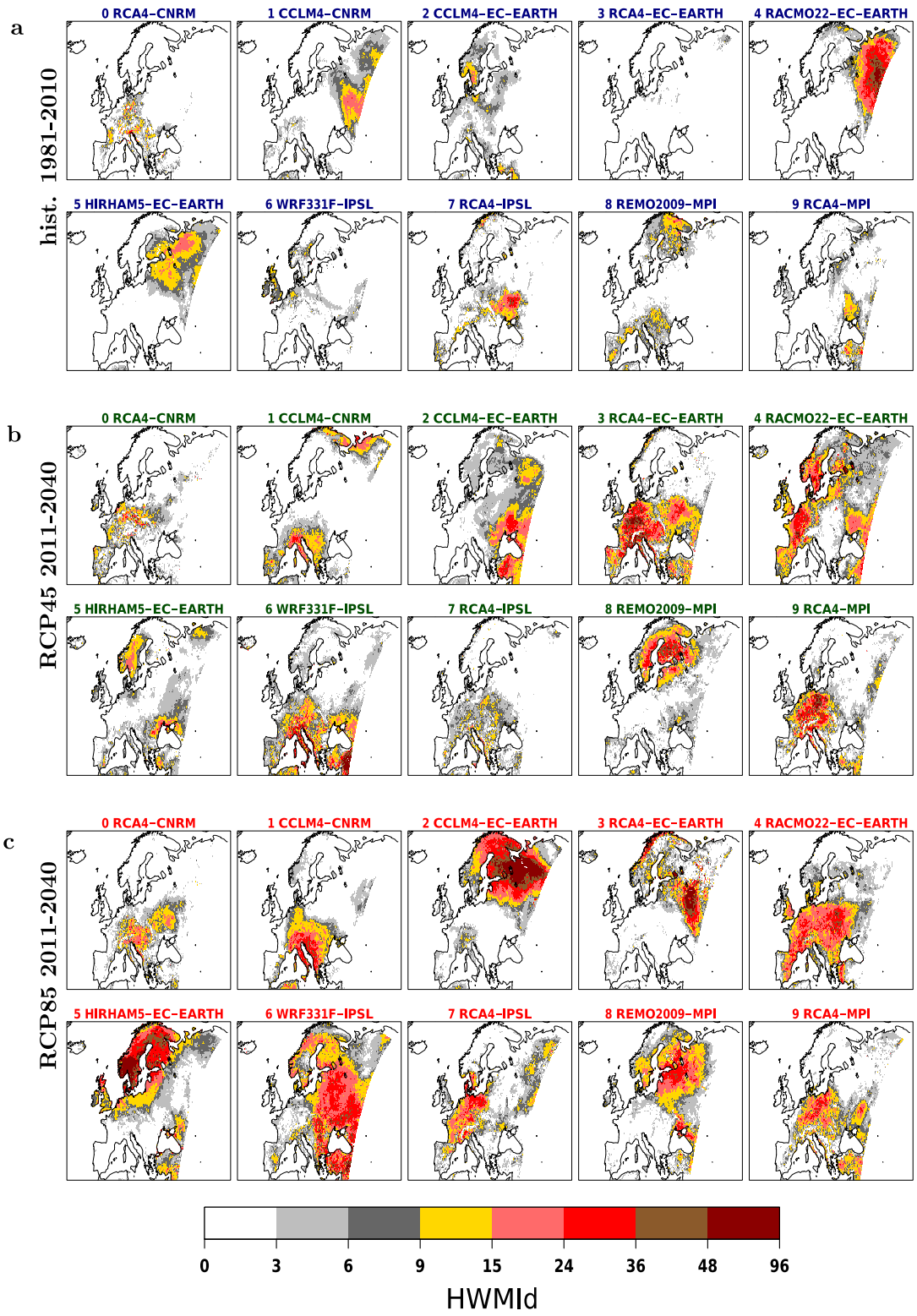

Figure A4. As figure 5 but for HWMId calculated with Tmin in the same model year of the strongest heatwaves represented in figure 5.

References

Alexander L V *et al* 2006 Global observed changes in daily climate extremes of temperature and precipitation *J. Geophys. Res.* **111** D05109

Barriopedro D *et al* 2011 The hot summer of 2010: redrawing the temperature record map of Europe *Science* **332** 220–4

Battisti D S and Naylor R L 2009 Historical warnings of future food insecurity with unprecedented seasonal heat *Science* **323** 240–44

Beniston M 2004 The 2003 heat wave in Europe: a shape of things to come? An analysis based on Swiss climatological data and model simulations *Geophys. Res. Lett.* **31** L02202

Beniston M *et al* 2007 Future extreme events in European climate: an exploration of regional climate model projections *Clim. Change* **81** 71–95

Christensen J H *et al* 2007 *Climate Change 2007: The Physical Science Basis, Contribution of Working Group I to the Fourth Assessment Report on the Intergovernmental Panel on Climate*

Change ed S Solomon *et al* (Cambridge: Cambridge University Press) ch 11, p 996
Christensen J H *et al* 2013 *Climate Change 2013: The Physical Science Basis. Contribution of Working Group I to the Fifth Assessment Report of the Intergovernmental Panel on Climate Change* ed T F Stocker *et al* (Cambridge: Cambridge University Press) ch 14, pp 1217–308
Christidis N, Gareth S J and Stott P A 2015 Dramatically increasing chance of extremely hot summers since the 2003 European heatwave *Nat. Clim. Change* **5** 46–50
Clark R T, Brown S J and Murphy J M 2006 Modeling Northern Hemisphere summer heat extreme changes and their uncertainties using a physics ensemble of climate sensitivity experiments *J. Clim.* **19** 4418–35
Collins M *et al* 2013 Long-term climate change: projections, commitments and irreversibility *Climate Change 2013: The Physical Science Basis. Contribution of Working Group I to the Fifth Assessment Report of the Intergovernmental Panel on Climate Change* ed T F Stocker *et al* (Cambridge: Cambridge University Press)
Coumou D and Robinson A 2013 Historic and future increase in the global land area affected by monthly heat extremes *Environ. Res. Lett.* **8** 034018
Diffenbaugh N S and Scherer M 2011 Observational and model evidence of global emergence of permanent, unprecedented heat in the 20th and 21st centuries *Clim. Change* **107** 615–24
Efron B 1979 The 1977 Reitz Lecture. Bootstrap methods: another look at the jackknife *Ann. Stat.* **7** 1–26
Fischer E, Beyerle U and Knutti R 2013 Robust spatially aggregated projections of climate extremes *Nat. Clim. Change* **3** 1033–8
Fischer E M and Schär C 2010 Consistent geographical patterns of changes in high-impact European heatwaves *Nat. Geosci.* **3** 398–403
Fischer E M, Seneviratne S I, Luthi D and Schar C 2007 Contribution of land-atmosphere coupling to recent European summer heat waves *Geophys. Res. Lett.* **34** L06707
Frich P *et al* 2002 Observed coherent changes in climatic extremes during the second half of the twentieth century *Clim. Res.* **19** 193–212
García-Herrera R *et al* 2010 A review of the European summer heatwave of 2003 *Crit. Rev. Environ. Sci. Technol.* **40** 267–306
Gilleland E and Katz R W 2011 New software to analyze how extremes change over time *Eos* **92** 13–4
Haylock M R, Hofstra N, Klein Tank A M G, Klok E J, Jones P D and New M 2008 A European daily high-resolution gridded dataset of surface temperature and precipitation *J. Geophys. Res.* **113** D20119
Hoag H 2014 Russian summer tops 'universal' heatwave index *Nature* **16**
Karl T R, Meehl G A, Peterson T C, Kunkel K E, Gutowski W J Jr and Easterling D R 2008 *Executive Summary in Weather and Climate Extremes in a Changing Climate* US Climate Change Science Program and the Subcommittee on Global Change Research, Washington, DC
Lass W, Haas A, Hinkel J and Jaeger C 2011 Avoiding the avoidable: towards a European heat waves risk governance *Int. J. Disaster Risk Sci.* **2** 1–4
Luterbacher J, Dietrich D, Xoplaki E, Grosjean M and Wanner H 2004 European seasonal and annual temperature variability, trends, and extremes since 1500 *Science* **303** 1499–503
Meehl G A and Tebaldi C 2004 More Intense, more frequent, and longer lasting heat waves in the 21st century *Science* **305** 994–7
Miralles D G *et al* 2014 Mega-heatwave temperatures due to combined soil desiccation and atmospheric heat accumulation *Nat. Geosci.* **7** 345–9
Näyha S 1981 Short and medium-term variations in mortality in Finland. A study on cyclic variations, annual and weekly periods and certain irregular variations in mortality in Finland during the period 1968–1972 *Scand. J. Soc. Med. Suppl.* **21** 1–01
Näyha S 2007 Heat mortality in Finland in the 2000s *Int. J. Circumpolar Health.* **66** 418–24
Perkins S E and Alexander L V 2013 On the measurement of heat waves *J. Climate* **26** 4500–17
Quesada B, Vautard R, Yiou P, Hirschi M and Seneviratne S 2012 Asymmetric European summer heat predictability from wet and dry Southern winters and springs *Nat. Clim. Chang.* **2** 736–41
Rahmstorf S and Coumou D 2011 Increase of extreme events in a warming world *Proc. Natl Acad. Sci. USA* **108** 17905–9
Robine J M, Cheung S L, Le Roy S, Van Oyen H, Griffiths C, Michel J P and Herrmann F R 2008 Death toll exceeded 70 000 in Europe during the summer of 2003 *C. R. Biologies* **331** 171–8
Russo S *et al* 2014 Magnitude of extreme heat waves in present climate and their projection in a warming world *J. Geophys. Res.* **119** D022098
Schär C *et al* 2004 The role of increasing temperature variability in European summer heatwaves *Nature* **427** 332–6
Sillmann J, Kharin V V, Zwiers F W, Zhang X and Bronaugh D 2013 Climate extreme indices in the CMIP5 multi-model ensemble: II. Future climate projections *J. Geophys. Res. Atmos.* **118** 2473–93
Stefanon M, D'Andrea F and Drobinski P 2012 Heatwave classification over Europe and the Mediterranean region *Environ. Res. Lett.* 7
Stott P A, Jones G S, Christidis N, Zwiers F, Hegerl G and Shiogama H 2011 Single-step attribution of increasing frequencies of very warm regional temperatures to human influence *Atmos. Sci. Lett.* **12** 220–7
Taylor K E, Stouffer R J and Meehl G A 2012 An Overview of CMIP5 and the Experiment Design *Bull. Am. Meteor. Soc.* **93** 485–98
Vautard R *et al* 2013 The simulation of European heat waves from an ensemble of regional climate models within the EURO-CORDEX preoject *Clim. Dyn.* **41** 2555–75
Vautard R, Yiou P, DAndrea F, de Noblet N, Viovy N, Cassou C, Polcher J, Ciais P, Kageyama M and Fan Y 2007 Summertime European heat and drought waves induced by wintertime Mediterranean rainfall deficit *Geophys. Res. Lett.* **34** L07711